Paper No. 949. (quote when citing this article)
Eleventh World Conference on Earthquake Engineering
ISBN: 0 08 042822 3

SOIL-STRUCTURE INTERACTION EFFECT ON THE EIGENPROPERTIES OF STRUCTURE

N. FUKUWA and M. A. GHANNAD

Department of Architecture, School of Engineering, Nagoya University
Furo-Cho, Chikusa-Ku, Nagoya 464-01, JAPAN

ABSTRACT

In order to grasp the effect of soil-structure interaction (SSI) on the dynamic characteristics of structure, the eigenproperties of a shear building model with uniform mass and stiffness distribution on surface of a homogeneous half-space are evaluated. As the evaluation method, two approaches are introduced : 1) Explicit representation of the determinant of the dynamic stiffness matrix using the cofactor expansion property, 2) Using the transfer matrix method to represent the transfer function explicitly. By using the cone models as an alternative to the rigorous solution for soil's impedance functions, the dependency of the soil-structure system's natural frequencies and damping ratios on the analysis model, number of stories, size of foundation and soil's stiffness are studied through the complex eigenvalue analysis. This is done for both, undamped and damped cases and it is clarified that the SSI has a large influence on the dynamic properties of structure. In this regard, the proper selection of damping model plays an important role.

KEYWORDS

Soil-Structure Interaction; Natural frequency; Damping Ratio; Radiation Damping; Cone Models; Cofactor Expansion; Transfer Matrix Method

INTRODUCTION

Contrary to the conventional assumption, the soil under the structure is not rigid and the interaction of the soil and stucture leads to a new system with different dynamic properties. This soil-structure system usually has a longer natural period than the fixed-base structure model. It also has a higher damping ratio, due to the radiation damping in the soil. Furthermore, soil-structure system is affected by additional mode shapes than those taken into account in the fixed-base model because of the sway and rocking degrees of freedom. The key aspect of any SSI analysis is the suitable modeling of the soil and calculating its dynamic stiffness. In this regard, as an alternative to rigorous solutions, cone models based on the one dimensional wave propagation theory can be used with sufficient accuracy for practical applications (Wolf, 1994). In this research, by using the cone models for homogeneous half-space (Wolf and Meek, 1992 and Meek and Wolf, 1993a), the effect of SSI on the dynamic properties of structure is investigated. Also investigated is the importance of proper damping modeling and its effect on the SSI results. Although this research is done for the foundation on the surface of a homogeneous half-space case, the cone models also allow the embedded and pile foundations even for a layered site to be analyzed (Wolf, 1994). Therefore, the method can be easily extended to the other above mentioned cases.

COFACTOR EXPANSION METHOD

Figure 1 shows the uniform distributed mass and stiffness shear building model which is chosen as the basic model in this research. In this model, each story is considered as a lumped mass with mass and mass moment of inertia of m and j, respectively. The total stiffness of each story is represented by a spring with stiffness of k and the material damping is considered as the hysteresis damping with damping ratio of h. The height of all the stories are assumed to be equal and represented by H. Additionally, the effect of soil is taken into account by introducing the translational and rotational springs and dashpots under the structure's foundation. The general free vibration equation of motion for this model will be as follows :

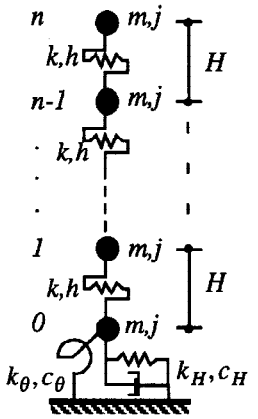

Fig.1. Analysis model

$$\begin{bmatrix} 1-\hat{\zeta}^2 & -1 & \cdots & 0 & 0 & -1 \\ -1 & 2-\hat{\zeta}^2 & & 0 & 0 & 0 \\ \vdots & & \ddots & \vdots & \vdots & \vdots \\ 0 & 0 & & 2-\hat{\zeta}^2 & -1 & 0 \\ 0 & 0 & \cdots & -1 & 1+\kappa_H\dfrac{1+2\zeta h_H i}{1+2hi}-\hat{\zeta}^2 & 1 \\ -1 & 0 & \cdots & 0 & 1 & \dfrac{k_\theta+i\omega c_\theta}{mH^2(1+2hi)\omega_0^{\,2}}+n-\dfrac{(n+1)j\hat{\zeta}^2}{mH^2} \end{bmatrix} \begin{Bmatrix} u_n \\ u_{n-1} \\ \vdots \\ u_1 \\ u_0 \\ \theta H \end{Bmatrix} = 0 \qquad (1)$$

where $\omega_0=\sqrt{k/m}$, $\zeta=\omega_n/\omega_0$, $\hat{\zeta}=\dfrac{\zeta}{\sqrt{1+2hi}}$, $\kappa_H=\dfrac{k_H}{k}$, $h_H=\dfrac{c_H\omega_o}{2k_H}$ (2)

The last two rows and columns of the coefficient matrix in the left-hand side of (1) are related to the sway and rocking degrees of freedom, respectively. So, the equations of motion for the sway-permitted and fixed-base cases can be easily obtained by deleting the last one or both of them, respectively. In each case, the complex eigenfrequencies of the n-story building will be computed by equating the determinant of the related stiffness matrix to zero. By cofactor expansion method, these determinants can be expressed in the following form for the fixed-base, sway-permitted and SR cases, respectively (Fukuwa *et al*, 1995).

$$f_n^{fix}(\zeta)=\left(1-\frac{\zeta^2}{1+2hi}\right)f_{n-1}^{tri}(\zeta)-f_{n-2}^{tri}(\zeta) \qquad (3)$$

$$f_n^{sway}(\zeta)=\left[\left(1+\kappa_H\frac{1+2\zeta h_H i}{1+2hi}\right)-\frac{\zeta^2}{1+2hi}\right]f_n^{fix}(\zeta)-f_{n-1}^{fix}(\zeta) \qquad (4)$$

$$f_n^{SR}(\zeta)=\left\{\left[\left(\kappa_H\kappa_\theta^{\,2}\frac{1+2\zeta h_\theta i}{1+2hi}+n\right)-\frac{(n+1)\kappa_m^{\,2}\zeta^2}{1+2hi}\right]f_n^{sway}(\zeta)-\left[\left(1+\kappa_H\frac{1+2\zeta h_H i}{1+2hi}\right)-\frac{\zeta^2}{1+2hi}\right]f_{n-1}^{tri}(\zeta)+\right.$$

$$\left.f_{n-2}^{tri}(\zeta)-f_n^{fix}(\zeta)+2\right\}H^2 \qquad (5)$$

where

$$f_n^{tri}(\zeta)=\frac{1}{2^n}\sum_{j=0}^{m}\frac{C_{2j+1}^{n+1}\zeta^{2j}}{(1+2hi)^j}\left(2-\frac{\zeta^2}{1+2hi}\right)^{n-2j}\left(\frac{\zeta^2}{1+2hi}-4\right)^j \qquad m = \text{quotient of } n \text{ and } 2 \qquad (6)$$

is the determinant of a tridiagonal submatrix which is obtained by deleting the first raw and column of the dynamic stiffness matrix for fixed-base case. In all above equations, the indices show the dimensions of the related matrices. Also, the other parameters are defined as follows :

$$\kappa_\theta=\frac{1}{H}\sqrt{\frac{k_\theta}{k_H}} \quad , \quad \kappa_m=\frac{1}{H}\sqrt{\frac{j}{m}} \quad , \quad h_\theta=\frac{c_\theta\omega_0}{2k_\theta} \qquad (7)$$

TRANSFER MATRIX METHOD

Figure 2 shows the basic perodic structure model and its fundamental structural element. The governing equation of motion of this model for unit support excitation is

$$\begin{Bmatrix} u_n \\ 0 \end{Bmatrix} = T^n \begin{Bmatrix} 1 \\ p_0 \end{Bmatrix} \tag{8}$$

where T is the transfer matrix for each fundamental structural element as bellow

$$T = \begin{bmatrix} 1-\beta^2 & -1/k^* \\ k^*\beta^2(2-\beta^2) & 1-\beta^2 \end{bmatrix} = \begin{bmatrix} \cos\varphi & -1/k^* \\ k^*\sin^2\varphi & \cos\varphi \end{bmatrix} \tag{9}$$

in which $$k^* = (1+2hi)k \quad , \quad \cos\varphi = 1-\beta^2 \quad , \quad \beta^2 = \frac{\omega^2}{2k^*/m} = \frac{\zeta^2}{2(1+2hi)} \tag{10}$$

Solving (8) easily leads to the response of each particle (i.e. the transfer function). Figure 3 shows the sway-permitted case in which the sway spring and dashpot are considered. Additionally, the mass $m/2$ is added to the particle 0 as well as the last particle in order to form a uniform distributed mass model. It should be mentioned that the fixed-base model can be considered as a limit case in which the stiffness and damping coefficients of

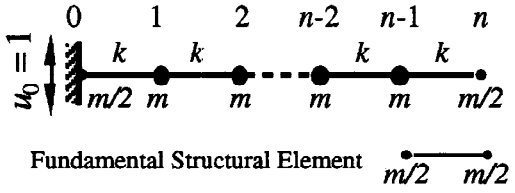

Fig. 2. Basic periodic structure model

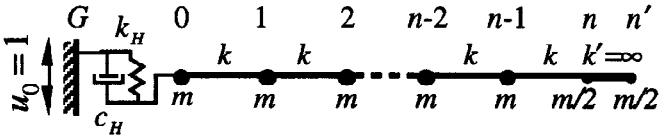

Fig. 3. Sway-permitted model

the spring and dashpot approaches infinity. After modifying the governing equation of motion, (8), for this condition, it leads to the following solutions for the fixed-base and sway-permitted cases, respectively (Fukuwa and Matsushima 1994 and Fukuwa *et al*, 1995).

$$u_l = \frac{\cos\frac{(2n-2l+1)}{2}\varphi}{\cos\frac{(2n+1)}{2}\varphi} \quad , \quad u_l = \frac{\kappa_H^* \cos\frac{(2n-2l+1)}{2}\varphi}{(\kappa_H^*-1)\cos\frac{(2n+1)}{2}\varphi + \cos\frac{(2n+3)}{2}\varphi} \qquad (l = 0,1,...,n) \tag{11}$$

where

$$\kappa_H^* = \frac{k_H + i\omega c_H}{k^*} = \kappa_H \frac{1+2h_H\zeta i}{1+2hi} \tag{12}$$

For the fixed-base model, the complex eigenfrequencies will be computed as follows by equating the denominator of the right-hand side of the related formula in (11) to zero

$$\varphi_{n,\alpha} = \frac{2\alpha-1}{2n+1}\pi \quad , \quad \omega_{n,\alpha} = \omega_0\sqrt{2(1+2hi)}\sqrt{1-\cos\left(\frac{2\alpha-1}{2n+1}\right)\pi} \qquad (\alpha = 0,1,...,n) \tag{13}$$

Also the eigenmodes can be calculated by introducing (13) in (11). So, it means that the natural frequencies, mode shapes and transfer functions can be obtained explicitly by using the transfer matrix method. However, unfortunately, for the sway-permitted case, the natural frequencies can not be represented explicitly.

RESULTS FOR A TYPICAL EXAMPLE

An ordinary RC rigid framed structure with square plan is used here as example to show the results more clearly. The number of stories, n, the number of spans, n_s (which is related to the foundation's dimensions directly) and the shear wave velocity of the soil, V_s, are selected as key parameters in this research and the other

parameters are fixed to the following numerical values :

m =1.2 t/m^2 , l=7 m , H=4.0 m , b=0.9 m , E=2.1x10^7 kN/m^2 , h=0.01 , ρ=1.8 t/m^3 , $\nu = 0.4$

which are belonged to the mass per unit area of each floor, the length of each span, dimension of the square columns, the modulus of elasticity, complex damping ratio in the structure, specific mass and the poisson's ratio in the soil, respectively. It should be noted that since the poisson's ratio in this numerical example is chosen greater than 1/3, the specific recommendations by Meek and Wolf (1993) is considered in relation to the cone models.

Undamped Case

First the damping effect isn't addressed and therefore a real eigenvalue analysis is done. Figure 4 shows the variation of the undamped circular frequencies with the number of stories, shear wave velocity of the soil and number of spans. In each figure, the results of the fixed-base, sway-permitted and SR models are shown as a nondimensionalized factor by dividing them by ω_0. Figures 4-a and 4-b show an obvious difference among different models, especially for lower modes of lower number of stories or softer soil. As the shear wave velocity of the soil increases, the differences between the sway-permitted and SR models with the fixed-base model decrease, as expected. Also Fig. 4-c shows that except for the first mode of SR model, the effect of SSI on the natural freqencies increases by increasing the number of spans. It means that generally the SSI effect is more important for larger size foundations, but it is necessary to consider the effect of rocking when the number of spans is too small. Since the first mode of vibration is usually the most important one, the variation of the first natural period of structure with the key parameters are presented in Fig. 5 for different base conditions. Again, the results are nondimensionalized by dividing by T_0, the natural period of the single degree of freedom system. Figure 5-a shows almost a linear relationship between the first natural period and the number of stories for the fixed-base and sway-permitted models. These linear relationships seem to be extented parallel to each other for larger number of stories. On the other hand, the relationship for the SR model is not linear and the

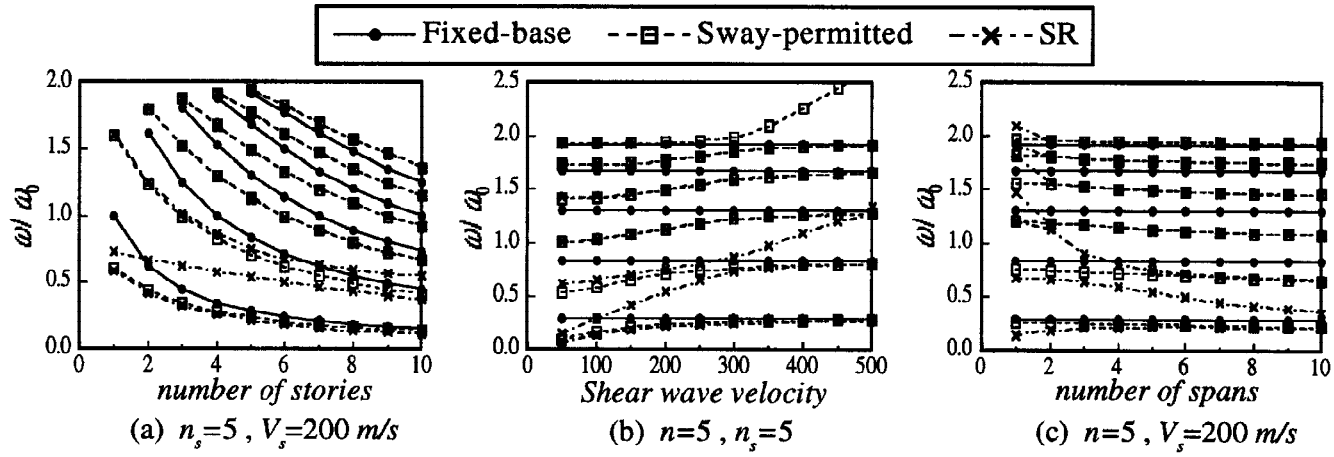

(a) n_s=5 , V_s=200 *m/s* (b) n=5 , n_s=5 (c) n=5 , V_s=200 *m/s*

Fig. 4. Undamped natural frequencies

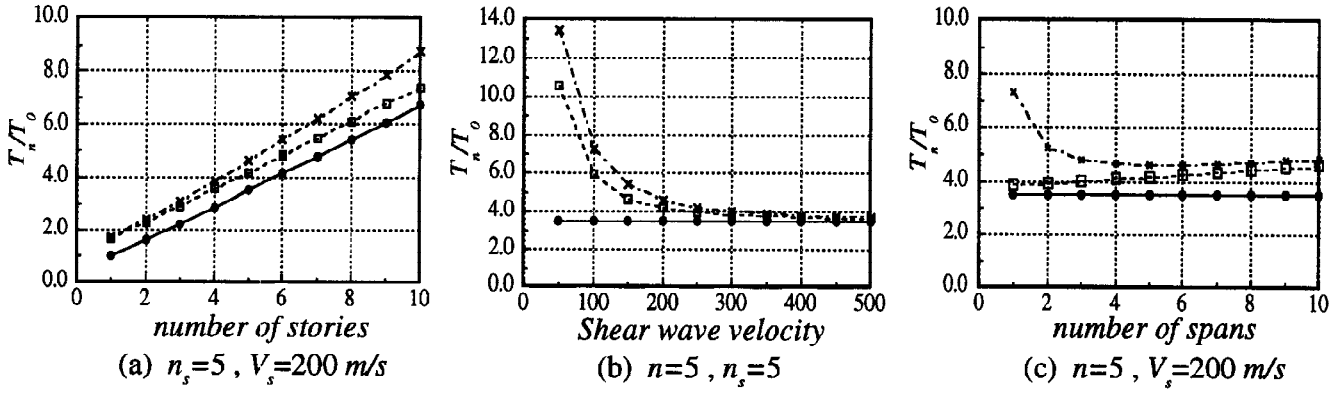

(a) n_s=5 , V_s=200 *m/s* (b) n=5 , n_s=5 (c) n=5 , V_s=200 *m/s*

Fig. 5. The first undamped natural periods

higher number of stories, the more necessity to considering the SSI effect. Figure 5-b is compatible with the fact that the results of the sway-permitted and SR models converge to those of the fixed-base model for high shear wave velocities of the soil. As concluded before, Fig. 5-c shows that rocking effect may be important for very small foundations. Also shown is the fact that although the sway-permitted case results are close to those of fixed-base model for low number of spans, the difference become larger as the number of spans increases.

Damped Case

In this section the damped case is considered and the natural frequencies and damping ratios are computed through the complex eigenvalue analysis. Figure 6 shows the relationship between the natural frequencies and damping ratios. Also Figs. 7 and 8 show the dependency of the natural frequencies and damping ratios on the

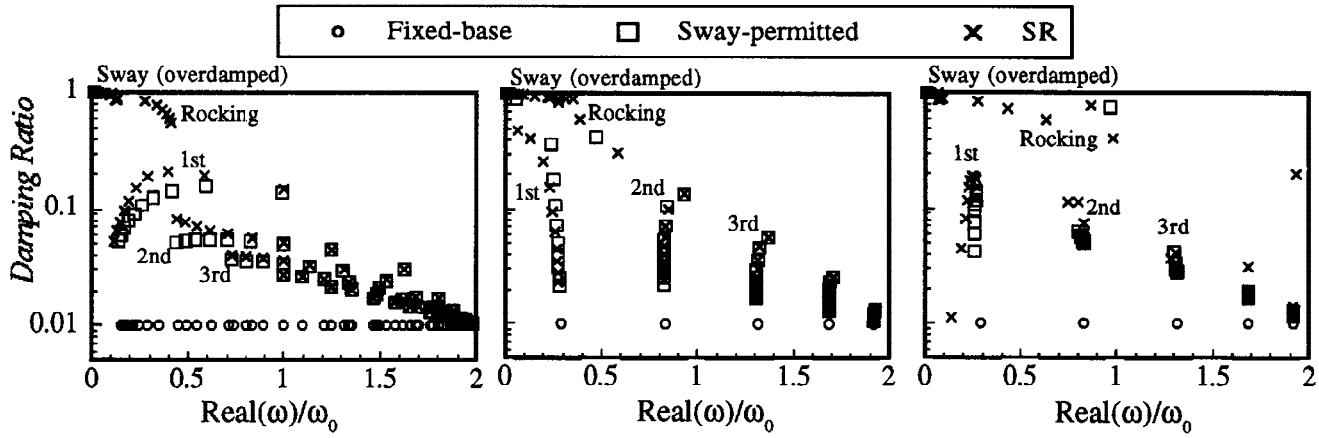

(a) n=1~10 , n_s=5 , V_s=200 *m/s* (b) n=5 , n_s=5 , V_s=50~500 *m/s* (c) n=5 , n_s=1~10 , V_s=200 *m/s*

Fig. 6. Modal damping ratios versus the natural frequencies

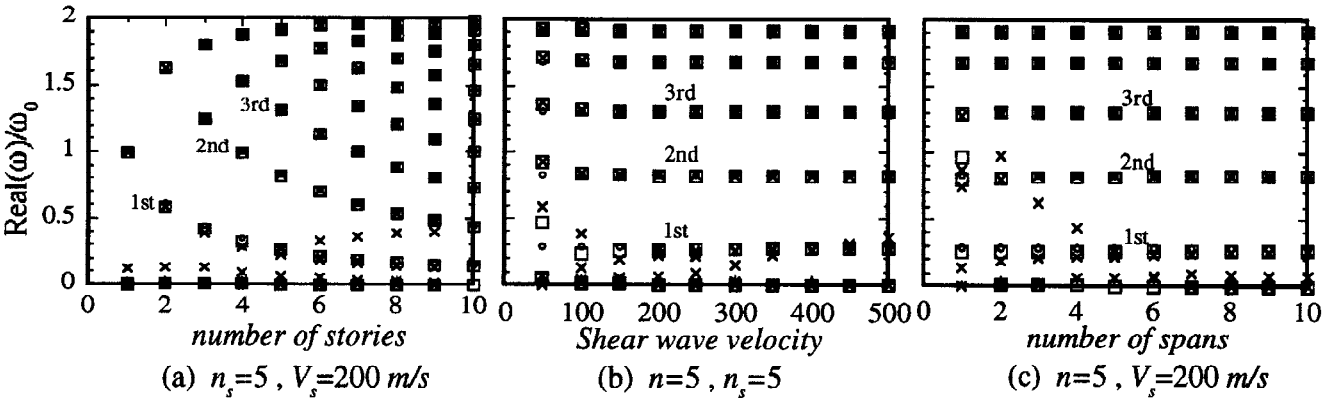

(a) n_s=5 , V_s=200 *m/s* (b) n=5 , n_s=5 (c) n=5 , V_s=200 *m/s*

Fig. 7. Damped natural frequencies

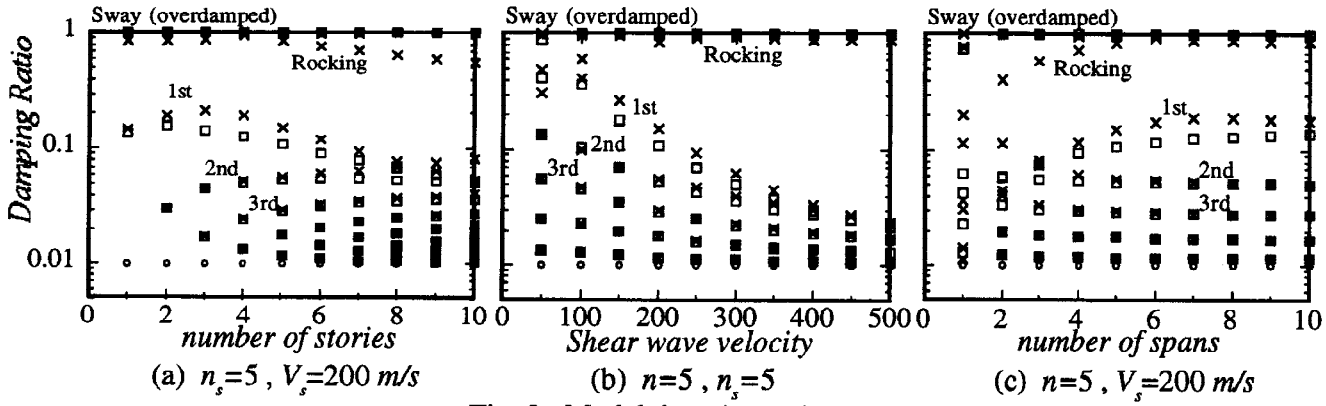

(a) n_s=5 , V_s=200 *m/s* (b) n=5 , n_s=5 (c) n=5 , V_s=200 *m/s*

Fig. 8. Modal damping ratios

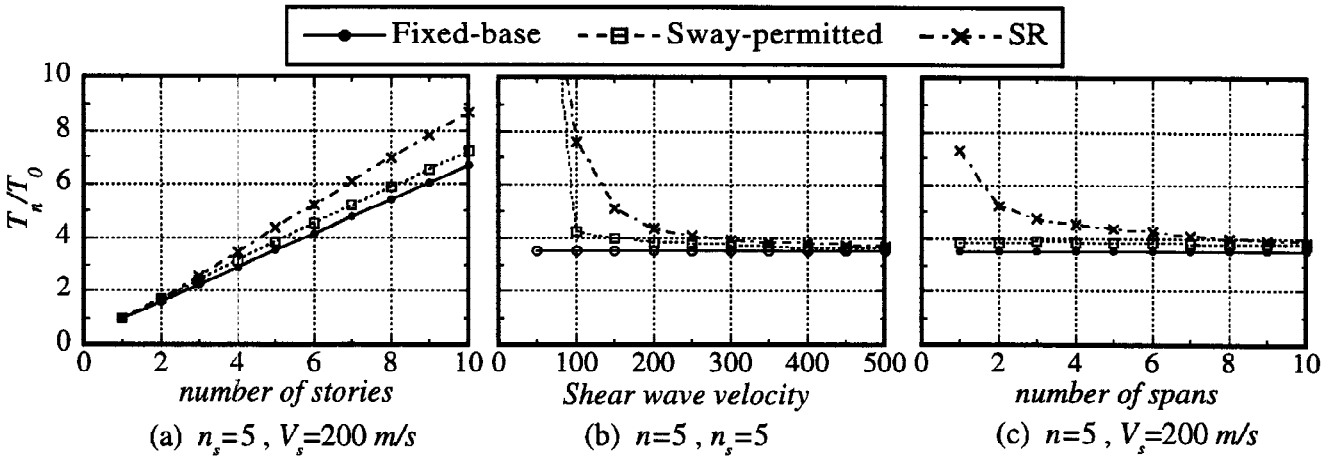

Fig. 9. The first natural period of structure in the damped case

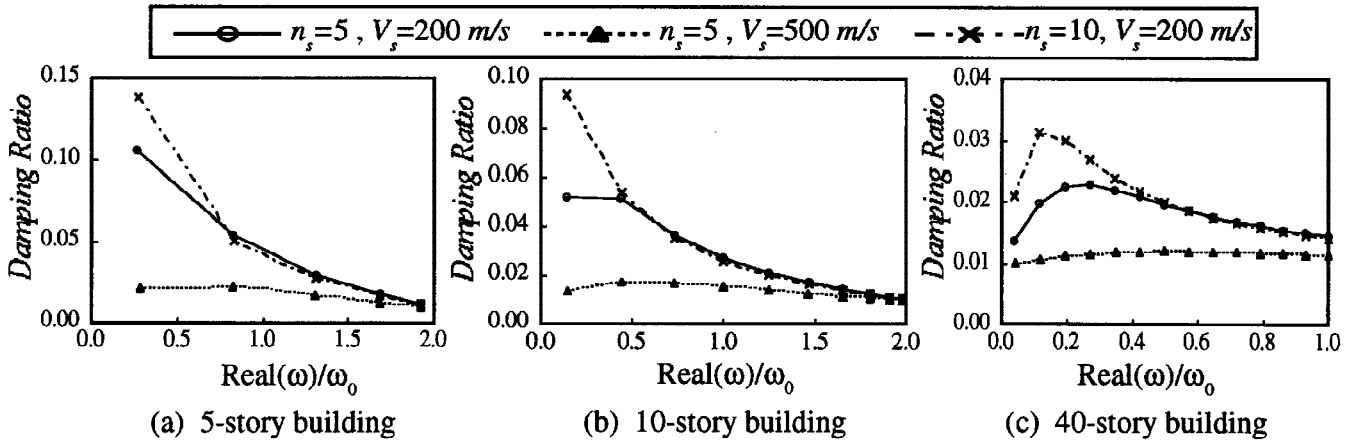

Fig. 10. The modal damping versus the natural frequencies for the sway-permitted case

key parameters in this research. In each figure, the results of three different base conditions are shown together. The comparison between Fig. 7 and Fig. 4 reveals that the resulted natural frequencies for damped and undamped cases are conceptually different. Figure 7 shows less difference among the fixed-base, sway-permitted and SR models. It seems that for complex analysis results, the difference among these different models are negligible for second and higher modes. Again as done for undamped case, the effect of SSI on the first natural period of models is shown in Fig. 9 which shows almost the same relationships and tendencies as Fig. 5. However, Fig. 9 shows less difference between the sway-permitted and SR models with fixed-base model. So, it can be concluded that SSI effect on the natural frequencies of structure will be overestimated in the case of real eigenvalue analysis. Additionally, the results for two additional modes, related to sway and rocking degrees of freedom, are completely different in the damped and undamped cases. It can be seen in Fig. 8 that the sway modes are generally overdamped. Also, the rocking modes are highly damped and the variation of the related natural frequencies is very high (Fig. 7). In relation to the damping ratio, Fig. 8 shows very high values for the first mode of structure which decrease for higher modes and finally converge to the material damping in the structure. This property is seen more clearly for lower shear wave velocities and higher number of spans, which is compatible with the fact that the radiation damping is higher for softer soil and larger foundations. In order to show the effect of SSI on the modal damping ratios more clearly, as a simple example, three models with different number of stories as symbols of short, moderate hight and highrise buildings are analyzed for different number of spans and shear wave velocities. The results for the sway-permitted model are shown in Fig. 10 as the damping ratio versus the natural frequency. It can be seen clearly that there are higher damping ratios for lower number of stories, lower shear wave velocities and higher number of spans. Although for the models with low and moderate number of stories the damping ratio decreases with the order of modes, for the 40-story model, it decreases after an initial increase. However, according to the some previous experimental studies (for example Tamura *et al*, 1994) the damping ratio generally increases with the order of the mode. The answer to

this variance lies in the fact that these kind of experimental data are mostly available only for highrise buildings where usually only the first few modes are achieved. So, they are compatible with the results shown in Fig. 10-c. Consequently, using the stiffness proportional damping model which leads to higher damping ratios for higher modes can not represent the SSI effect properly.

Results of The Transfer Matrix Method

In this section by using the transfer matrix method, the effect of SSI is detected through the construction of transfer function for a base excitation case. Figure 11 shows the n-th particle's response for the fixed-base and sway-permitted models according to (11). For showing the effect of the damping model on the natural frequency

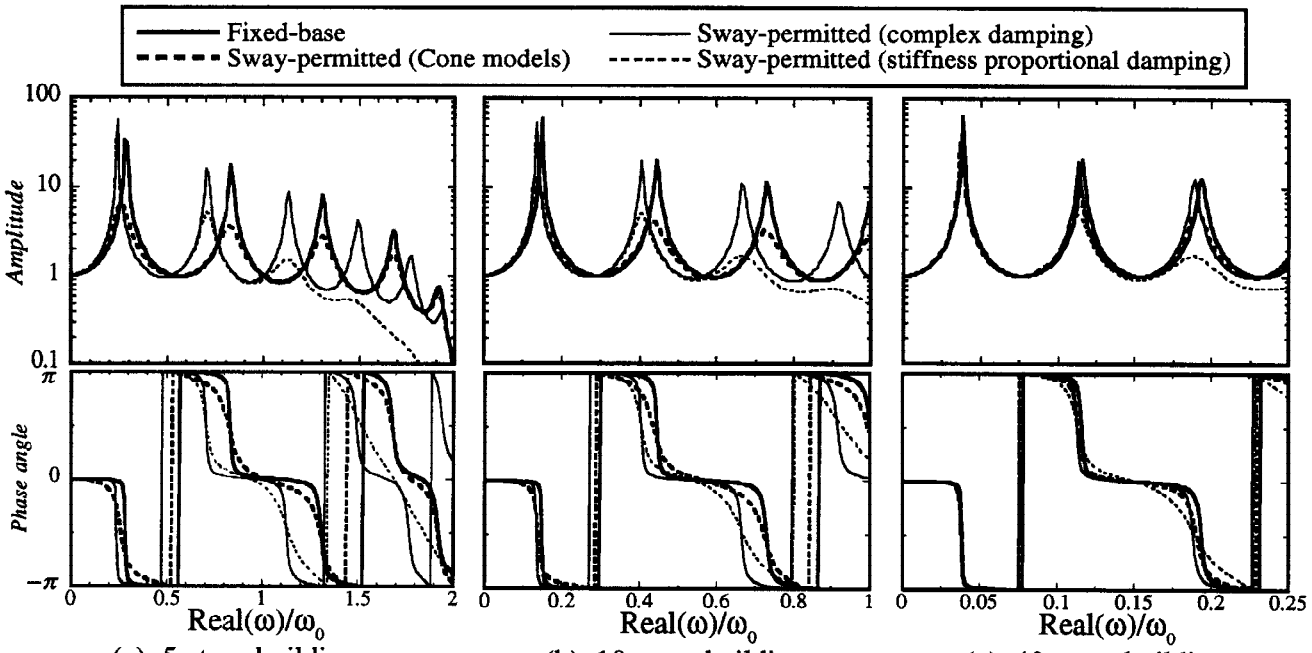

(a) 5-story building (b) 10-story building (c) 40-story building

Fig. 11. Transfer function and phase angle for the last story (n_s=5 , V_s=200 *m/s*)

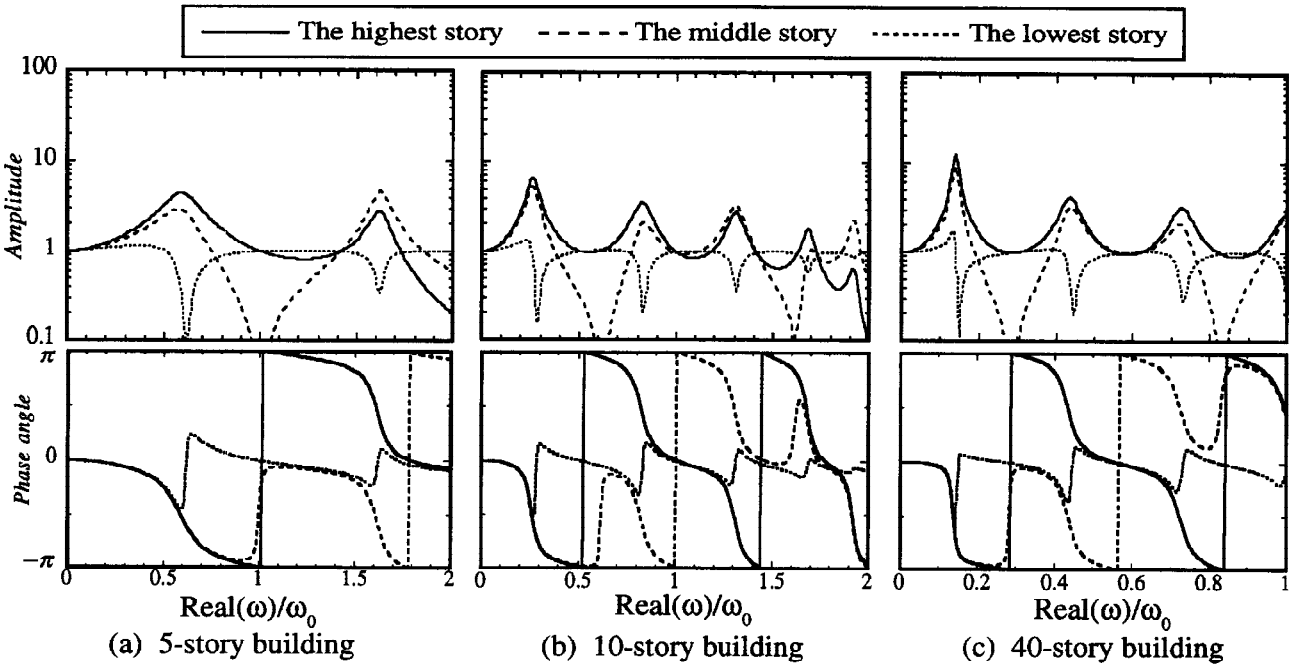

(a) 5-story building (b) 10-story building (c) 40-story building

Fig. 12. Transfer function and phase angle for different parts of building (n_s=5 , V_s=200 *m/s*)

results, two other damping models are used for sway-permitted case. As the first model, a constant complex damping of 1% is considered for the soil as in the structure, which leads to a system of uncoupled differential equations. The other one is considered as a stiffness proportional damping model for whole the system with the damping ratio of 1% in the first mode. It can be seen in Fig. 11 that for the sway-permitted case with use of cone model, the frequencies related to the peak values are very close to thoes of fixed-base model. However, the two other models estimate these frequencies to be much less. Additionally, the stiffness proportional damping model underestimates the peak values related to the second and higher modes because of high damping ratios for higher modes. These effects can be seen more clearly for structures with low and moderate height.

From another point of view, Fig. 12 shows the response of the lowest, the middle and the highest part of the building in the sway-permitted case using cone model. As it can be seen, there is a phase difference between the different parts of the building and the structure actually vibrates with a phase delay. This means that using damping models, such as proportional damping models, which lead to the real eigenmodes can not be a suitable approach.

CONCLUSION

In order to grasp the SSI effect on the dynamic properties of structure, a shear building model accompanied by sway and rocking springs and dashpots based on the cone models' impedance functions was used and the following results were achieved :

The effect of SSI on the natural frequencies of structure is not so high and especially diminishes for the second and higher modes. However, the SSI effect on the damping ratio is considerable especially for those modes whose natural frequencies are closer to those of the sway and rocking modes. This effect is higher for lower number of stories, larger foundations and softer soil.

The damping models which lead to the real eigenvalue analysis, underestimate the natural frequencies of the system and can not be a suitable choice. Attention to this point is more important for lower number of stories.

Although for the first modes of tall buildings the damping ratio increases for higher modes, generally the higher modes have lower damping ratios. This can be seen clearly for low and moderate number of stories and also for higher modes of highrise buildings after the initial increase. This means using the stiffness proportional damping model which leads to higher damping ratios for the higher modes can not be a suitable approach.

REFERENCES

Fukuwa, N. and S. Matsushima (1994). Wave dispersion and optimal mass modeling for one dimensional periodic structures. *Earthquake Eng. Str. Dyn.*, Vol. **23**, pp. 1165-1180

Fukuwa, N. and M.A. Ghannad and S. Yagi (1995). A study on the effect of soil-structure interaction on the eigenproperties of structure. *J. Str. Const. Eng., Transactions of Architectural Inst of Japan (AIJ)*, No. **475**, pp. 35-44 (In Japanese)

Meek,W. and J. P. Wolf (1993). Cone models for nearly incompressible soil. *Earthquake Eng. Str. Dyn.*, Vol. **22**, pp. 649-663

Meek,W. and J.P. Wolf (1993a). Why cone models can represent the elastic half-space. *Earthquake Eng. Str. Dyn.*, Vol. **22**, pp. 759-771

Tamura, Y. and M. Yamada and H. Yokota (1994). Estimation of structural damping of buildings. *ASCE Structures Congress XII*, pp. 1012-1027

Wolf, J.P. and W. Meek (1992). Cone models for homogeneous soil. I. *ASCE, J. Geotech. Eng.*, Vol. **118**, No. 5, pp. 667-685

Wolf, J.P. (1994). *Foundation vibration analysis using simple physical models.* Prentice Hall, Englewood cliffs, N.J.